

Infinite Randomness Fixed Point in the Dissipative Random Transverse Field Ising Model

Gr  gory Schehr and Heiko Rieger
Theoretische Physik Universit  t des Saarlandes 66041 Saarbr  cken Germany
(Dated: December 2, 2024)

The interplay between disorder, quantum fluctuations and dissipation is studied in the random transverse Ising chain coupled to a dissipative Ohmic bath with a real space renormalization group. A quantum phase transition at zero temperature is found that is described by an infinite randomness fixed point. In the Griffiths-McCoy region away from the critical point frozen clusters produce already a finite magnetization resulting in a classical behavior of the susceptibility. These override the confluent singularities characterized by a continuously varying dynamical exponent and originating in the non-frozen strongly coupled clusters.

PACS numbers: 75.10.Nr, 75.40.-s, 05.30.Jp, 05.10.Cc

The presence of quenched disorder in a quantum mechanical system may have drastic effects in particular close to and at a quantum critical point. The appearance of a Griffiths-McCoy singularities [1, 2], leading to the divergence of various quantities like the susceptibility at zero temperature even far away from a quantum critical point, has received considerable attention recently [3, 4, 5, 6, 7]. This quantum Griffiths behavior is characteristic for quantum phase transitions described by an infinite randomness fixed point (IRFP) [8], which was shown to be relevant for many disordered quantum systems [9].

Quantum Griffiths behavior was proposed to be the physical mechanism responsible for the “non-Fermi-liquid” behavior observed in many heavy-fermion materials [10, 11]. However, recently it was argued that in a dissipative environment, as in metals due to the conduction electrons, such a quantum Griffiths behavior might essentially be non-existent [12]. Moreover, even the underlying sharp quantum phase transition itself was shown to be rounded in dissipative model systems [13]. Obviously there is a need to examine carefully the effect of dissipation on a quantum system displaying IRFP and quantum Griffiths behavior in the non-dissipative case and to treat correctly the mixing of critical and Griffiths-McCoy singularities — which is what we intend to do in this letter.

The properties of a single spin coupled to a dissipative bath has been extensively examined [14]. Upon increasing the coupling strength between spin and bath degrees of freedom it displays at zero temperature a transition from a non-localized phase, in which the spin can still tunnel, to a localized phase, in which tunneling ceases and the spin behaves classically. Such a transition is also present in an infinite ferromagnetic spin chain coupled to a dissipative bath, as was shown recently numerically [15]. Here we want to focus on the interplay of disorder, quantum fluctuations and dissipation and study the Random Transverse Field Ising chain (RTIC) where each spin is coupled to an ohmic bath of harmonic oscillators [16]. It is defined on a chain of length L with periodic boundary conditions (p.b.c.) and described by the Hamiltonian H :

$$H = \sum_{i=1}^L \left[-J_i \sigma_i^z \sigma_{i+1}^z - h_i \sigma_i^x + \sum_{k_i} \frac{p_{k_i}^2}{2} + \omega_{k_i} \frac{x_{k_i}^2}{2} + C_{k_i} x_{k_i} \sigma_i^z \right] \quad (1)$$

where $\sigma_i^{x,z}$ are Pauli matrices and the masses of the oscillators are set to one. The quenched random bonds $J_i \geq 0$ (respectively random transverse field $h_i \geq 0$) are uniformly distributed between 0 and J_0 (respectively between 0 and h_0). The properties of the bath are specified by its spectral function $J_i(\omega) = \frac{\pi}{2} \sum_{k_i} C_{k_i}^2 / \omega_{k_i} \delta(\omega - \omega_{k_i}) = \frac{\pi}{2} \alpha_i \omega e^{-\omega/\Omega_i}$ where Ω_i is a cutoff frequency. Initially the spin-bath couplings and cutoff frequencies are site-independent, i.e. $\alpha_i = \alpha$ and $\Omega_i = \Omega$, but both become site-dependent under renormalization.

To characterize the ground state properties of this system (1), we follow the idea of a real space renormalization group (RG) procedure introduced in Ref. [17] and pushed further in the context of the RTIC without dissipation in Ref. [3]. The strategy is to find the largest coupling in the chain, either a transverse field or a bond, compute the ground state of the associated part of the Hamiltonian and treat the remaining couplings in perturbation theory. The bath degrees of freedom are dealt with in the spirit of the “adiabatic renormalization” introduced in the context of the (single) spin-boson model [14], where it describes accurately its critical behavior [18].

Suppose that the largest coupling in the chain is a transverse field, say h_2 . Before we treat the coupling of site 2 to the rest of the system $-J_1\sigma_1^z\sigma_2^z - J_2\sigma_3^z\sigma_3^z$ perturbatively as in [3] we consider the effect of the part $-h_2\sigma_2^x + \sum_k(p^2/2 + \omega_k x_k^2/2 + C_k x_k \sigma_2^z)$ of the Hamiltonian, which represents a single spin-boson model. For this we integrate out frequencies ω_k that are much larger than a lower cut-off frequency $ph_2 \ll \Omega_2$ with the dimensionless parameter $p \gg 1$. Since for those oscillators $\omega_k \gg h_2$ one can assume that they adjust instantaneously to the current value of σ_2^z the renormalized energy splitting is easily calculated within the adiabatic approximation [14] and one gets an effective transverse field $\tilde{h}_2 < h_2$:

$$\tilde{h}_2 = h_2 (ph_2/\Omega_2)^{\alpha_2} \quad , \quad \tilde{\Omega}_2 = ph_2 \quad . \quad (2)$$

If \tilde{h}_2 is still the largest coupling in the chain the iteration (2) is repeated. Two situations may occur depending on the value of α_2 . If $\alpha_2 < 1$ this procedure (2) will converge to a finite value $h_2^* = h_2(p\tilde{h}_2/\Omega_2)^{\alpha_2/(1-\alpha_2)}$ and the spin-boson system at site 2 is in a delocalized phase in which the spin and the bath can be considered as being decoupled (formally $\alpha_2 = 0$), as demonstrated by an RG treatment in [18].

If this value h_2^* is still the largest coupling in the chain it

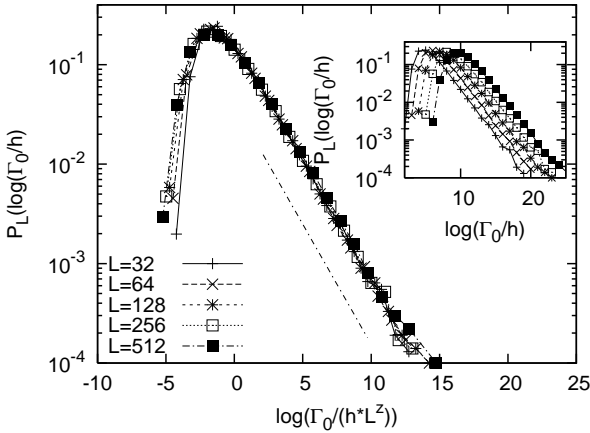


FIG. 1: $P_L(\log(\Gamma_0/h))$ as a function of $\log(\Gamma_0/hL^z)$ for different system sizes for $\alpha = 0.03$, *i.e.* far from the critical point ($h_0 = 1$, $J_0 = 0.34$). The straight line, has slope $1/z$ with $z = 1.65(5)$. **Inset** : $P_L(\log(\Gamma_0/h))$ as a function of $\log(\Gamma_0/h)$ for different system sizes L for $\alpha = 0.03$. The same symbols are used as in the main figure.

will be aligned with the transverse field. As in the RTIC without dissipation, this spin is then decimated (as it will not contribute to the magnetic susceptibility) and gives rise, in second order degenerate perturbation theory, to an effective coupling \tilde{J}_1 between the neighboring moments at site 1 and 3 [3]

$$\tilde{J}_1 = J_1 J_2 / h_2^* \quad (3)$$

If $\alpha_2 > 1$, \tilde{h}_2 can be made arbitrarily small by repeating the procedure (2) implying that the spin-boson system on site 2 is in its localized phase [18] and essentially behaves classically: the decimation rule (2) indeed amounts to set $\tilde{h}_2 = 0$. Such a moment, or cluster of spins, will be aligned with an infinitesimal external longitudinal field and is denoted as “frozen”.

Suppose now that the largest coupling in the chain is a bond, say J_2 . The part of the Hamiltonian that we focus on is $-J_2 \sigma_2^z \sigma_3^z + \sum_{i=1,2} \sum_{k_i} (p_i^2/2 + \omega_{k_i} x_{k_i}^2/2 + C_{k_i} x_{k_i} \sigma_i^z)$, *i.e.* a subsystem of two spin-bosons coupled via J_2 . We find that in second order perturbation theory the ground state of this subsystem is equivalent to a single spin-boson system coupled to *both* baths leading to the additive rule

$$\tilde{\alpha}_2 = \alpha_2 + \alpha_3 \quad (4)$$

Integrating out the degrees of freedom of both baths with frequencies larger than pJ_2 (as done previously for the single spin-boson system) one obtains that the two moments at 2 and 3 are replaced by a single moment $\tilde{\mu}_2$ with an effective transverse field \tilde{h}_2 :

$$\tilde{h}_2 = \frac{h_2 h_3}{J_2} \left(\frac{p J_2}{\Omega_2} \right)^{\alpha_2} \left(\frac{p J_2}{\Omega_3} \right)^{\alpha_3} \quad (5)$$

$$\tilde{\mu}_2 = \mu_2 + \mu_3, \quad \tilde{\Omega}_2 = p J_2 \quad (6)$$

where μ_i is the magnetic moment of site i (in the original model, one has $\mu_i = 1$ independently of i). Combining Eq. (4) and Eq. (6) one clearly sees that $\tilde{\alpha}_i = \tilde{\mu}_i \alpha$.

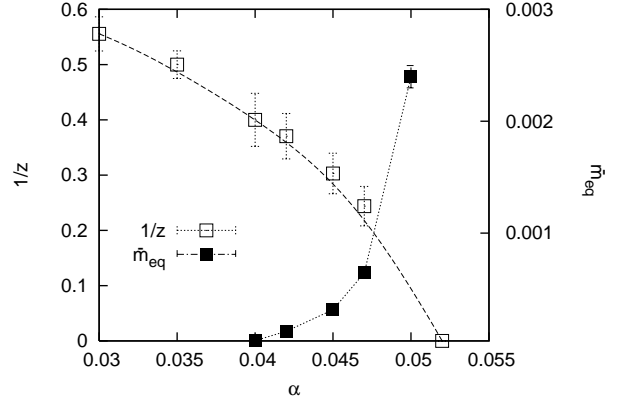


FIG. 2: Inverse dynamical exponent $1/z$ and magnetization m_{eq} as a function of α (for $h_0 = 1$, $J_0 = 0.34$)

In the following we analyze this RG procedure defined by the decimation rules (2-6) numerically. This is done by considering a finite chain of size L with p.b.c. and iterating the decimation rules until only one site is remaining. This numerical implementation has been widely used in previous works [9], and it has been shown in particular to reproduce with good accuracy the exact results of Ref. [3] for the RTIC. We fix $h_0 = 1$ and concentrate on the parameter plane (α, J_0) . All data were obtained by averaging over 10^5 different disorder realizations (if not mentioned otherwise), and the disorder average of an observable O is denoted \overline{O} . The decimation rules (2-6) depend explicitly on the “ad hoc” parameter p (or more precisely on the ratio Ω/p). For the moment we fix $\Omega/p = 10^4$ and discuss the weak dependence on this parameter below. The following data are obtained for $J_0 = 0.34$.

The transverse field h acting on the last remaining spin that is not frozen is an estimate for the smallest excitation energy in the ensemble of non-localized spins. Its distribution $P_L(\log(h))$, where Γ_0 is the largest coupling in the initial chain of size L , reflects the characteristics of the gap distribution in the dissipationless case [6]. The inset of Fig. 1 shows $P_L(\log(h))$ for $\alpha = 0.03$. For a system close to, but not at, a quantum critical point described by an IRFP one expects indications of Griffiths-McCoy singularities characterized by the following scaling behavior for P_L

$$P_L(\log(h)) = \mathcal{P}(\log(hL^z)), \quad (7)$$

where z is a dynamical exponent that depends on the distance to the critical point. Fig. 1 shows a good data collapse with $z = 1.65$ for the chosen coupling constant $\alpha = 0.03$. The slope of the dotted line in Fig. 1 is identical to $1/z$ and one observes that by repeating these calculations for increasing values of α the slope, *i.e.* $1/z$ decreases. The numerical estimates for $1/z(\alpha)$ for different values of α are shown in Fig. 2; they indicate that $1/z$ approaches zero for some critical value α_c , which implies formally $z \rightarrow \infty$ for $\alpha \rightarrow \alpha_c$. This is also characteristic for an IRFP and we expect to find a critical value for α_c ,

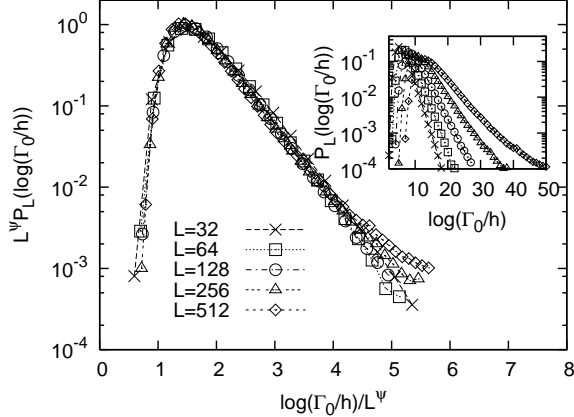


FIG. 3: $P_L(\log(\Gamma_0/h))$ as a function of $\log(\Gamma_0/hL^\psi)$ for different system sizes for $\alpha = 0.052$. **Inset** : $P_L(\log(\Gamma_0/h))$ as a function of $\log(\Gamma_0/h)$ for different system sizes L for $\alpha = 0.052$. The same symbols are used as in the main figure

where $P_L(\log(\Gamma_0/h))$ displays the following scaling behavior:

$$P_L(\log(\Gamma_0/h)) = L^{-\psi} \mathcal{P}_{\text{IRFP}}(L^{-\psi} \log(\Gamma_0/h)), \quad (8)$$

where ψ is a critical exponent characterizing the IRFP. Fig. 3 shows $P_L(\log(\Gamma_0/h))$ for $\alpha = 0.052$: In the inset one observes that it broadens systematically with increasing system size, in contrast to the data shown in the inset of Fig. 1, and the main plot displays a good data collapse according to (8) with $\psi = 0.32$. When we vary α slightly, the data collapse according to (8) gets worse, therefore we take $\alpha_c = 0.052$ as our estimate for the critical point (for $h_0 = 1$ and $J_0 = 0.34$) and denote by $\delta = (\alpha_c - \alpha)/\alpha_c$ the distance from the critical point.

The magnetic moment μ of the last remaining spin in the decimation procedure represents an estimate of the total magnetization $m_{\text{eq}}L$ of the chain. In Fig. 4, we show $\alpha\bar{\mu}(L)$ as a function of L for different values of δ . For small L , $\mu(L) \propto L^a$ with $a \simeq 1/3$ up to a length scale $L^* \sim O(10^4)$ beyond which the effective coupling between strongly coupled clusters and the bath, $\alpha\mu$, gets larger than one and the clusters become localized. Above this value $\mu(L) \sim \bar{m}_{\text{eq}}L$ (see inset of Fig. 4), which suggests a finite magnetization \bar{m}_{eq} before the critical point is reached. This is a manifestation of the “frozen” clusters and lead to the concept of rounded quantum phase transitions in the presence of dissipation [13]. The typical size of a frozen cluster turns out to be rather large, here larger than $L^* \sim 10^4$, below which quantum Griffiths behavior prevails.

Due to the localized frozen clusters magnetic order is still short ranged below α_c , long range order only sets in at the IRFP, where the average correlation function $\bar{C}(r)$ decays algebraically. We compute it by keeping track of the clusters during the decimation procedure and define

$$C(r) = L^{-1} \left(\sum_i w_{i,i+r} \right) - \bar{m}_{\text{eq}}^2 \quad (9)$$

where $w_{i,j} = 1$ if the sites i and j belong to the same cluster, and $w_{i,j} = 0$ otherwise. $\bar{C}(r)$ is then obtained by averaging

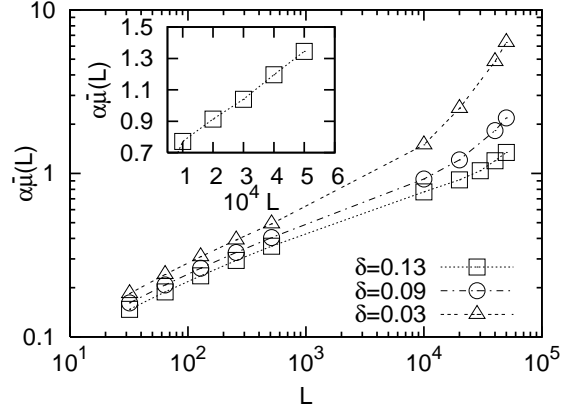


FIG. 4: Magnetic moment $\alpha\bar{\mu}(L)$ as a function of the system size L for different values of δ . **Inset** : $\alpha\bar{\mu}(L)$ for $L \geq 10^4$ as a function of L and for $\delta = 0.13$. The linear behavior suggests a finite \bar{m}_{eq} . The lines are guides to the eyes. Due to the large system sizes the data are averaged only over 500 different disorder realizations.)

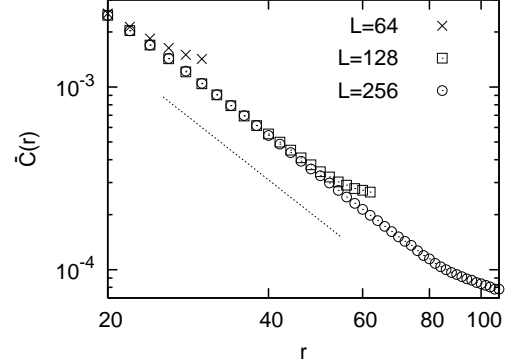


FIG. 5: Log-log plot of the correlation function $\bar{C}(r)$ as a function of r for different system sizes L for $\alpha = 0.052$. The straight line corresponding to $r^{-2.2}$ is a guide to the eyes. Error-bars are smaller than the sizes of the symbols.

over 10^6 different realizations of the random couplings. We have checked that for RTIC without dissipation at the critical point this gives the correct exponent [3] within 5% accuracy. In Fig. 5, we show $\bar{C}(r)$ as defined in Eq. (9) for different system sizes at $\delta = 0$, i.e. at the IRFP. The data fit well to

$$\bar{C}(r) \sim r^{-\beta}, \quad \beta = 2.2(1) \quad (10)$$

To estimate the correlation length exponent we also characterize the approach to the critical point by performing a finite size scaling analysis. The inset of Fig. 6 shows $\bar{C}(L/2)$ for different values of δ . One expects the scaling behavior

$$\bar{C}(L/2) = L^{-\beta} F(L\delta^\nu) \quad (11)$$

and we get a good data collapse, as shown in Fig. 6, with $\nu = 1.25$ (and the value $\beta = 2.2$ as estimated above).

An IRFP is characterized by the 3 independent exponents ψ , β and ν [8]. Our numerical RG analysis gives $\psi = 0.32(2)$,

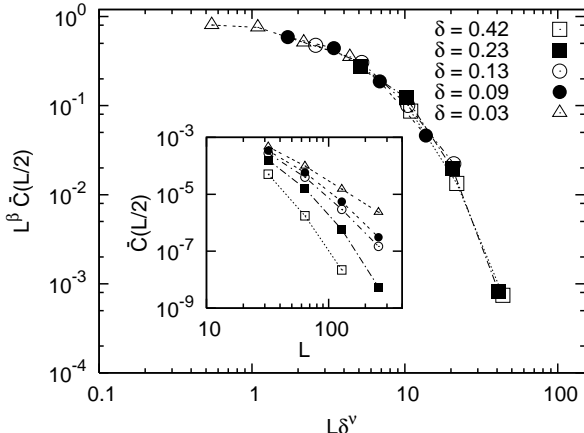


FIG. 6: $L^{2.2}\bar{C}(L/2)$ as a function of $L\delta^v$ for different values of δ , with $v = 1.25(5)$. Error-bars are smaller than the sizes of the symbols. Inset : $\bar{C}(L/2)$ as a function of L for different values of δ , with the same symbols as in the main figure.

$\beta = 2.2(1)$ and $v = 1.25(5)$ (the error margins for ψ and v are estimated from the range of estimates where the scaling collapse is still acceptable, and for β from the range of exponents that still fit \bar{C} well). These values are clearly different from the values for the RTIC without dissipation: There $\psi_{\text{RTIC}} = 1/2$, $\beta_{\text{RTIC}} = (3 - \sqrt{5})/2 \simeq 0.38$ and $v_{\text{RTIC}} = 2$ [3].

We have checked that the dependence of the critical behavior characterized by Eq. (8,10,11) on the *ad hoc* parameter Ω/p in the range $10 - 10^4$ is very weak. In this range, the relative variations of the estimated critical exponents are of the order of 5%, although the value of the critical point α_c is more sensitive, and probably non universal.

We repeated the previous analysis for different values of J_0 (keeping $h_0 = 1$) and identified the critical point by varying α . This allows to determine the phase diagram in the (α, J_0) plane, which is depicted in Fig. 7. Our estimates for the critical exponents ψ , β and v vary only weakly along the critical line, their relative variation being less than 10%. We suggest that the critical behavior along the line except the end points, is determined by a unique IRFP, different from the one describing the RTIC without dissipation at $(\alpha = 0, J_0 = 1)$, and different from the single spin-boson model $(\alpha = 1, J_0 = 0)$.

To conclude our strong disorder RG study of the random transverse Ising chain coupled to a dissipative Ohmic bath provided evidence for a sharp quantum phase transition at a critical coupling strength and the existence of quantum Griffiths behavior close to it. The transition looks rounded when looking at the magnetization, which is positive already in the paramagnetic phase, in agreement with [13], but it is well defined by a diverging spatial correlation length and IRFP scaling behavior only at the critical point. The frozen clusters producing the non-vanishing magnetization in the Griffiths region give rise to a classical T^{-1} divergence of the susceptibility, as predicted by [12], which overrides confluent Griffiths-McCoy singularities characterized by a continuously varying dynam-

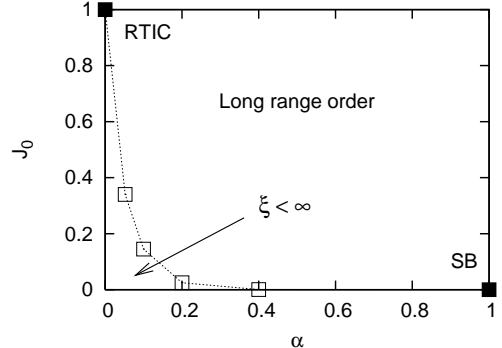


FIG. 7: Phase diagram for $h_0 = 1$, and $\Omega/p = 10^4$.

ical exponent $z(\alpha)$ and contributing only a $T^{-1+1/z(\alpha)}$ to the susceptibility. Our RG treatment shows that quantum Griffiths behavior can actually be observed up to a rather large crossover length scale ($L \geq 10^4$), beyond which the classical behavior of the frozen clusters sets in. This implies, on one hand, that numerical studies can hardly track the asymptotic behavior [16] and, on the other hand, that experiments at very low but non-vanishing temperatures might still show indications for quantum Griffiths behavior [10, 12]. In higher dimensions we also expect an IRFP and quantum Griffiths behavior, and it would be interesting to extend our study to Heisenberg antiferromagnets and XY systems.

GS acknowledges the financial support provided through the European Community's Human Potential Program under contract HPRN-CT-2002-00307, DYLAGEMEM.

- [1] R. B. Griffiths, Phys. Rev. Lett. **23**, 17 (1969).
- [2] B. M. McCoy, Phys. Rev. Lett. **23**, 383 (1969); Phys. Rev. **188**, 1014 (1969).
- [3] D. S. Fisher, Phys. Rev. Lett. **69**, 534 (1992); Phys. Rev. B **51**, 6411 (1995).
- [4] M. J. Thill and D. A. Huse, Physica A **214**, 321 (1995).
- [5] H. Rieger and A. P. Young, Phys. Rev. B **54**, 3328 (1996); M. Guo, R. N. Bhatt and D. A. Huse, Phys. Rev. B **54**, 3336 (1996).
- [6] F. Iglói and H. Rieger, Phys. Rev. B **57**, 11404 (1998).
- [7] C. Pich *et al.*, Phys. Rev. Lett. **81**, 5916 (1998).
- [8] D. Fisher, Physica A **263**, 222 (1999); O. Motrunich *et al.*, Phys. Rev. B **61**, 1160-1172 (2000).
- [9] For a recent review, see F. Iglói and C. Monthus, Phys. Rep. **412**, 277 (2005).
- [10] M. C. Andrade *et al.*, Phys. Rev. Lett. **81**, 5620 (1998); A. H. Castro Neto, G. Castilla, and B. A. Jones, Phys. Rev. Lett. **81**, 3531 (1998).
- [11] G. R. Stewart, Rev. Mod. Phys. **73**, 797 (2001).
- [12] A. J. Millis, D. K. Morr, and J. Schmalian, Phys. Rev. Lett. **87**, 167202 (2001); Phys. Rev. B **66**, 174433 (2002);
- [13] T. Vojta, Phys. Rev. Lett. **90**, 107202 (2003).
- [14] A. Leggett *et al.*, Rev. Mod. Phys., **59**, 1 (1987).
- [15] P. Werner *et al.*, Phys. Rev. Lett. **94**, 047201 (2005).
- [16] L. F. Cugliandolo, G. S. Lozano, and H. Lozza, Phys. Rev. B **71**, 224421 (2005).
- [17] S.K.Ma, C. Dasgupta and C.K. Hu, Phys. Rev. Lett. **43**, 1434 (1979); C. Dasgupta and S.K. Ma, Phys. Rev. B **22**, 1305 (1980).
- [18] R. Bulla *et al.*, Phys. Rev. B **71**, 045122 (2005).